Measurement of NH Bond Lengths by Fast Magic-Angle Spinning Solid-State NMR Spectroscopy: A New Method for the Quantification of Hydrogen Bonds

Xin Zhao,[†] James L. Sudmeier,[‡] William W. Bachovchin,[‡] and Malcolm H. Levitt*[,†,§]

Physical Chemistry Division, Arrhenius Laboratory Stockholm University, S-106 91 Stockholm, Sweden
Biochemistry Department, Tufts University 136 Harrison Avenue, Boston, Massachusetts 02111
Chemistry Department, University of Southampton Southampton SO17 1BJ, United Kingdom

Received June 1, 2001

Hydrogen bonding plays a very important role in a wide range of molecular structures and mechanisms.[1,2] Unfortunately, hydrogen bonds are difficult to quantify by X-ray crystallography because of the low scattering cross-section of hydrogen atoms. As a result, NMR methods for the site-resolved study of hydrogen bonding are very important sources of information.

In a recent communication,[3] some of us described a new solid-state NMR method for the efficient recoupling of heteronuclear dipole−dipole interactions in the presence of fast magic-angle-spinning. This allows the high-precision measurement of heteronuclear bond lengths with good chemical shift resolution in multiply isotopically labelled systems. In this communication, we apply this method to the measurement of $^{15}N-^{1}H$ bond lengths in crystalline [U-^{13}C,^{15}N]-L-histidine·HCl·H_2O. We detect a clear elongation of one of the imidazole NH bonds, due to the formation of an intermolecular hydrogen bond. This establishes the method as a powerful tool for investigating hydrogen bonding in macromolecules, including enzymes, membrane proteins, and fibers. The experiment does not require high-quality crystals or specific isotropic labelling and is feasible on systems which are unsuitable for solution NMR because of their large molecular size or tendency to aggregate.

The method is based on recently developed symmetry theorems for selective recoupling and decoupling in magic-angle-spinning solid-state NMR.[4] We exploit the rotor-synchronized sequence $R18_2^5$, which consists of a repetitive sequence of $180_{50}180_{-50}$ pulse pairs, where β_ϕ denotes a pulse of flip angle β and phase ϕ (in degree), and the duration of each 180° pulse is equal to $^1/_9$ of a rotational period. As shown elsewhere,[3] this symmetry leads to the suppression of isotropic chemical shifts and homonuclear dipolar couplings, while the heteronuclear dipolar couplings and the chemical shift anisotropies (CSA) of the irradiated nuclei are recoupled.

If the $R18_2^5$ sequence is applied at the ^1H Larmor frequency, then the ^{15}N spectrum of $^{15}N-^{1}H$ groups displays a splitting due to the recoupled heteronuclear dipolar interactions. The $^{15}N-^{1}H$ distance may be estimated from these splittings, since the dipolar coupling is proportional to the inverse cube of the distance. The formation of a $^{15}N-^{1}H\cdots O$ hydrogen bond elongates the $^{15}N-^{1}H$ bond and reduces the dipolar splitting. The extent of the elongation is anticipated to correlate with the hydrogen-bond energy.

Hydrogen-bond induced changes in the heteronuclear dipolar couplings have previously been studied by static solid-state NMR[5] and by spinning sideband analyses at rather slow MAS frequencies.[6] However, these methods do not provide optimal chemical shift resolution on multiply labelled samples and are of limited applicability. There are several other methods for heteronuclear dipolar recoupling at high MAS frequencies,[7−12] but none of these combine γ-encoded[13] heteronuclear recoupling with exact suppression of homonuclear dipole−dipole interactions in the first-order average Hamiltonian. Isotropic chemical shifts,[14,15] chemical shift anisotropies,[16,17] and homonuclear dipolar couplings[18] provide complementary information on hydrogen bonding.

In the $P2_12_12_1$ crystal structure of L-histidine hydrochloride monohydrate,[19] there is an intermolecular H-bond between the hydrogen atom of the $N(\delta_1)-H$ group and the carboxyl oxygen of a neighboring molecule (shown in Figure 1). In this communication, we use $R18_2^5$ recoupling to compare the lengths of the $N(\delta_1)-H$ and $N(\epsilon_2)-H$ bonds in a polycrystalline [U-^{13}C,^{15}N]-L-histidine·HCl·H_2O sample.

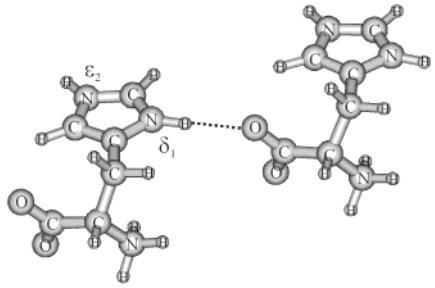

Figure 1. The crystal structure of L-histidine·HCl·H_2O (ref 19), showing the intermolecular hydrogen bond (Cl^- ions and H_2O molecules are omitted).

The two-dimensional separated local field pulse sequence is shown in Figure 2. Cross-polarized ^{15}N magnetization is allowed to evolve for a variable interval t_1 in the presence of $R18_2^5$ irradiation of the protons. The t_1 interval consists of increasing number of pairs of 180° pulses, so that the last t_1 increment

* To whom correspondence should be addressed.
† Stockholm University.
‡ Tufts University.
§ University of Southampton.

(1) Jeffrey, G. A.; Saenger, W. *Hydrogen Bonding In Biological Structures*; Springer-Verlag: Berlin, 1991.
(2) Desiraju, G. R.; Steiner, T. *The Weak Hydrogen Bond in Structural Chemistry and Biology*; Oxford University Press: New York, 1999.
(3) Zhao, X.; Edén, M.; Levitt, M. H. *Chem. Phys. Lett.* **2001,** *342*, 353−361.
(4) Carravetta, M.; Edén, M.; Zhao, X.; Brinkmann, A.; Levitt, M. H. *Chem. Phys. Lett*. **2000,** *321*, 205−215.
(5) Hoelger, C. G.; Limbach, H. H. *J. Phys. Chem.* **1994**, *98*, 11803−11810.
(6) Kimura, H.; Shoji, A., Sugisawa, H.; Deguchi, K., Naito, A.; Saito, H. *Macromolecules* **2000**, *33*, 6627−6629.
(7) Gross, J. D.; Costa, P. R.; Griffin, R. G. *J. Chem.. Phys*. **1998**, *108* , 7286−7293.
(8) Saalwachter, K.; Graf, R.; Spiess, H. W. *J. Magn. Reson.* **1999**, *140*, 471−476.
(9) van Rossum, B.-J.; de Groot, C. P.; Ladizhansky, V.; Vega, S.; de Groot, H. J. M. *J. Am. Chem. Soc*. **2000**, *122*, 3465−3472.
(10) Hohwy, M.; Jaroniec, C. P.; Reif, B.; Rienstra, C. M.; Griffin, R. G. *J. Am. Chem. Soc*. **2000**, *122*, 3218−3219.
(11) De Paul, S. M.; Saalwachter, K.; Graf, R.; Spiess, H. W. *J. Magn. Reson*. **2000**, *146*, 140−156.
(12) Chan, J. C. C. *Chem. Phys. Lett.* **2001**, *335*, 289−297.
(13) Nielsen, N. C.; Bildsøe, H.; Jakobsen, H. J.; Levitt, M. H. *J. Chem. Phys.* **1994**, *101*, 1805−1812.
(14) Wei, Y.; McDermott, A. E. In *Modeling NMR Chemical Shifts*: *Gaining Insights into Structure and Environment*; Facelli, J., de Dios, A. C., Eds.; American Chemical Society: Washington, DC, 1999; pp 177−193.
(15) Kamienski, B.; Schilf, W.; Dziembowska, T.; Rozwadowski, Z.; Szady-Chelmieniecka, A. *Solid State NMR* **2000**, *16*, 285−289.
(16) Wei, Y.; de Dios, A. C.; McDermott, A. E. *J. Am. Chem. Soc.* **1999**, *121*, 10389−10394.
(17) Wei, Y.; Lee, D.; Ramamoorthy, A. *J. Am. Chem. Soc*. **2001**, *123*, 6118−6126.
(18) Brown, S. P.; Zhu, X. X.; Saalwachter, K.; Spiess, H. W. *J. Am. Chem. Soc*. **2001**, *123*, 4275−4285.
(19) Fuess, H.; Hohlwein, D.; Mason, S. A. *Acta Crystallogr*. **1977**, *B33*, 654−659.

10.1021/ja016328p CCC: $20.00
Published on Web 10/12/2001

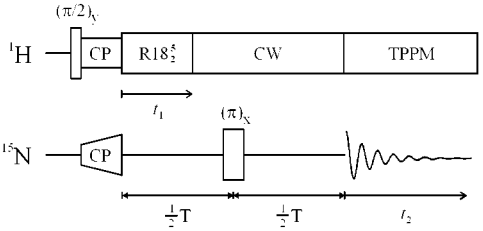

Figure 2. Two-dimensional constant−interval pulse sequence for heteronuclear dipolar recoupling using $R18_2^5$ in the t_1 dimension.

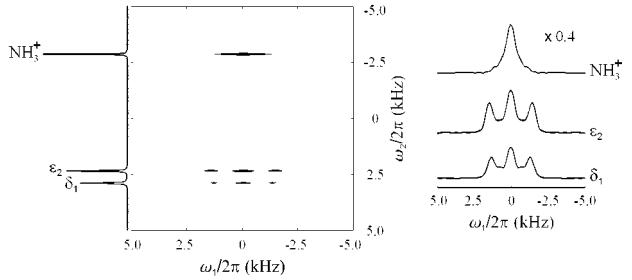

Figure 3. Experimental 2D ^{15}N spectrum of [U-^{13}C,^{15}N]-L-histidine·HCl·H_2O at a spinning frequency $\omega_r/2\pi = 20.000$ kHz, using the $R18_2^5$ sequence with a rf field of 90.0 kHz. To the left of the 2D spectrum is the 1D ^{15}N CP/MAS spectrum at the same spinning frequency. Sections through the 2D spectrum parallel to the ω_1 axis are shown on the right. The scale of the frequency axes respects the negative magnetogyric ratio of ^{15}N.[21] The NH_3^+ slice is displayed with a reduced vertical scale. The experiments were performed on a Varian CMX Infinity-400 instrument at a magnetic field of 9.4T using a 3.2 mm zirconia rotor. The ^{15}N chemical shifts of the δ_1 and ϵ_2 site are 142.2 and 128.8 ppm, respectively, with respect to the $^{15}NH_3^+$ site (see Supporting Information).

comprises 16 complete $R18_2^5$ sequences. Proton decoupling is then applied for an interval $(T/2 - t_1)$, where T is an even number of rotor periods, so that the total interval $T/2$ is kept constant as t_1 is increased. A 180° pulse is applied to the ^{15}N-spins, and ^{1}H-decoupled evolution continues for another interval $T/2$ before the ^{15}N-spin signal is acquired in the presence of TPPM decoupling.[20] This "constant-interval" procedure eliminates the modulation due to ^{15}N CSA, ^{15}N−^{15}N dipolar and J-coupling interactions. The 2D data matrix $s(t_1, t_2)$ is subjected to a cosine Fourier transformation in the t_1 domain and a complex Fourier transformation in the t_2 domain. The resulting 2D spectrum $S(\omega_1, \omega_2)$ contains pure absorption peaks.

A ^{15}N 2D dipolar-shift correlation spectrum of [U-^{13}C,^{15}N]-L-histidine·HCl·H_2O is shown in Figure 3. Each of the N(δ_1) and N(ϵ_2) nitrogens have one directly bonded proton and the recoupled spectra display a three-peak feature in the ω_1 dimension, as described in ref 3.

Projections of the N(δ_1)−H and N(ϵ_2)−H spectra in the ω_1 dimension are shown on an expanded scale in Figure 4 ,a and b. There is a perceptible difference in the dipolar splitting. Numerically exact two-spin simulations of the two peaks are shown in Figure 4, c and d. In the case of the ^{15}N(δ_1)−^{1}H bond, the best match with experiment is obtained with a NH bond length of 109 pm, while for the ^{15}N(ϵ_2)−^{1}H bond, the best match with experiment is obtained with a NH bond length of 105 pm. The effects of long-range couplings, proton chemical shifts, and rf field errors are documented in the Supporting Information.

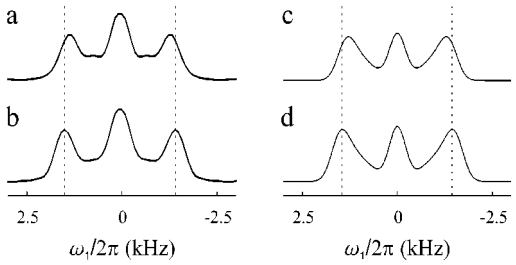

Figure 4. Sections though the 2D spectrum for the **(a)** ^{15}N(δ_1)−^{1}H and **(b)** ^{15}N(ϵ_2)−^{1}H groups. **(c)** and **(d)** Numerically exact simulations for an isolated ^{15}N−^{1}H group, using a direct ^{15}N−^{1}H coupling of $b_{IS}/2\pi = 9.41$ kHz, and 10.52 kHz, respectively. ^{1}H chemical shift anisotropy of $\delta^{aniso} = -1.0$ ppm, $\eta = 0$, and a Gaussian lineboardening with a width of 500 Hz was included in (c) and (d). The dashed lines are visual aids.

Table 1. NH Bond Lengths in L-Histidine·HCl·H_2O

	nitrogen site	*n*-diffraction[19]	present work
NH bond	ϵ_2	102.6 ± 0.4	105.0 ± 5.0
length r (pm)	δ_1	107.0 ± 0.4	109.0 ± 5.0
$r(\delta_1) - r(\epsilon_2)$		4.4 ± 0.8	4.0 ± 1.0

Table 1 shows the neutron diffraction data for the two N−H bonds in L-histidine·HCl·H_2O.[19] Neutron diffraction and solid-state NMR both show a ~4 pm elongation of the N(δ_1)−H bond relative to the N(ϵ_2)−H bond, although the absolute bond lengths estimated by the two methods are slightly different. This is due to the averaging of the N−H internuclear interaction by librational motion perpendicular to the bond direction.[22] Note that the confidence limits for the *difference* in the two NH distances are much tighter than for the absolute distances (see Supporting Information).

In the neutron diffraction study of L-histidine·HCl·H_2O,[19] the 4 pm elongation of the N(δ_1)−H bond is attributed to the strong intermolecular H-bond. This paper shows that the latest heteronuclear recoupling sequences are capable of detecting such bond length distortions with good chemical shift resolution on multiply labelled systems. The structural information is displayed as an easily interpreted splitting, allowing ready comparison of bond lengths between different chemical sites. We anticipate numerous applications to protein−ligand interactions and other structural and mechanistic problems.

It should also be possible to investigate C−H hydrogen bonds, which have been postulated to play a role in certain enzymatic processes.[23]

Acknowledgment. The research was supported by the Swedish Natural Science Research Foundation and by the Göran Gustafsson Foundation for Research in the Natural Science and Medicine. We thank Mattias Edén and Ole Johannessen for computational and instrumental help, and M. Hursthouse and A. Russell for discussions.

Supporting Information Available: Discussion of the ^{15}N chemical shifts and exploration of the effects of long-range dipolar couplings, isotropic proton chemical shifts, proton chemical shift anisotropies, and rf field errors on the line shapes (PDF). This material is available free of charge via the Internet at http://pubs.acs.org.

JA016328P

(20) Bennett, A. E.; Rienstra, C. M.; Auger, M.; Lakshmi, K. V.; Griffin, R. G. *J. Chem. Phys.* **1995**, *103*, 6951−6958.
(21) Levitt, M. H. *J. Magn. Reson.* **1997**, *126*, 164−182.
(22) Case, D. A. *J. Biomol. NMR* **1999**, *15*, 95−102.
(23) Ash, E. L.; Sudmeier, J. L.; Day, R. M.; Vincent, M.; Torchilin, E. V.; Haddad, K. C.; Bradshaw, E. M.; Sanford, D. G.; Bachovchin, W. W. *Proc. Natl. Acad. Sci. U.S.A.* **2000**, *97*, 10371−10376.